

Sputtering of Silicon Surface during Low-Energy High-Dose Implantation with Silver Ions

V. V. Vorob'ev^{a,b,*}, A. M. Rogov^{a,b}, V. I. Nuzhdin^b, V. F. Valeev^b, and A. L. Stepanov^b

^a Interdisciplinary Center Analytic Microscopy, Kazan Federal University, Kazan, 420008 Russia

^b Kazan Zavoisky Physical Technical Institute, Federal Scientific Center KazNTs,
Russian Academy of Sciences, Kazan, 420029 Russia

*e-mail: Slavik.Ksu@mail.ru

Received April 7, 2019; revised February 3, 2020; accepted February 10, 2020

Abstract—We report on the results of first practical observations of sputtering of the Si surface during the implantation with Ag^+ ions with an energy of 30 keV depending on irradiation dose D in the interval from 2.5×10^{16} to 1.5×10^{17} ion/cm² for a fixed value of ion beam current density $J = 8 \mu\text{A}/\text{cm}^2$, as well as for variation of $J = 2, 5, 8, 15,$ and $20 \mu\text{A}/\text{cm}^2$ at constant $D = 1.5 \times 10^{17}$ ion/cm². In the former case, the thickness of the porous Si (PSi) layer being sputtered increases monotonically to 50 nm at the maximum value of D ; in this case, the effective sputtering ratio of the implanted Ag : PSi layer is 1.6. We have also established that the thickness of the sputtered layer increases with current density J .

DOI: 10.1134/S1063784220070269

INTRODUCTION

The conversion of solar energy into electric energy is performed at present using commercial cells consisting of thick crystalline silicon wafers (c -Si) with a thickness from 180 to 300 μm [1]. The expenditures in manufacturing of solar cells are mainly determined by the cost of growing and subsequent technological processing of such thick-layer c -Si substrates. For this reason, the obtaining of solar cells on thin (less than 1 μm) Si layers with amorphous or polycrystalline structure is a topical and economically important problem [2, 3]. Light thin-layer solar cells can be integrated with modern compact optoelectronic microchips and Si-based devices and, hence, can find application in aerospace industry.

The main limitation for effective application of thin-film solar cells is the low absorption in the visible optical range near the edge of the fundamental band of a non-direct-gap semiconductor (Si). To increase the absorbability of Si-based solar cells, an approach has been proposed relatively recently in which small (<30 nm) nanoparticles of noble metals are included in the structure [4, 5]; in such nanoparticles, localized plasmon resonance appears under the action of light. Such a resonance of nanoparticles is manifested in intense absorption of light by metal nanoparticles in the ultraviolet, visible, and near-infrared spectral ranges [6, 7], which provides the total contribution to intensified absorption of the thin semiconducting

layer containing nanoparticles [8]. In addition, the local electromagnetic field induced in the vicinity of nanoparticles due to the plasmon resonance can generate electron–hole pairs in semiconductors [5]. In this case, Ag nanoparticles in Si-based solar cells are considered as most promising as regards the effectiveness of the plasmonics excitation and selective absorption in the visible optical range [9].

Composite Si-layers with Ag nanoparticles are formed using various methods, such as atmospheric laser evaporation [10], vacuum deposition of metals [11], and various chemical approaches [12]. Ion implantation technology, which is actively used in industrial Si microelectronics, is of special interest. The implantation of c -Si with ions such as B^+ and P^+ changes the type of Si conductivity, improves their photovoltaic properties, which is used in developing solar cell elements [13, 14]. However, no investigations devoted to the synthesis of nanoparticles of noble metals into the Si matrix during ion implantation for applications in solar power engineering have been performed.

We have recently proposed a new technology for the formation of thin porous Si layers with Ag nanoparticles (Ag : PSi) during low-energy high-dose ($>10^{16}$ ion/cm²) implantation of c -Si with Ag^+ ions (Ag : Si) [15, 16]. It was shown in these publications that during the implantation of c -Si with Ag^+ ions having low energy $E = 30$ keV and high dose $D = 1.5 \times$

10^{17} ion/cm², effective sputtering of the semiconductor surface occurs simultaneously with the synthesis of Ag nanoparticles and the formation of the porous P*Si* structure. In spite of the fact that considerable attention is paid in the scientific literature to Si sputtering during ion implantation (see, for example, reviews [17, 18]), information on the type of Si sputtering associated specifically with the heavy Ag⁺ ion is not available. In this study, we perform, for the first time, quantitative experiments on low-energy ion sputtering of Si depending on current density J in the ion beam and irradiation dose D during the implantation with Ag⁺ ions.

1. EXPERIMENTAL TECHNIQUE

As substrates for ion implantation, we used monocrystalline *c*-Si wafers with the (100) crystallographic orientation. The implantation was carried out with Ag⁺ ions having energy $E = 30$ keV for different doses D in the interval from 1.5×10^{15} to 1.5×10^{17} ion/cm² at constant current density $J = 8$ μ A/cm², as well as for fixed $D = 1.5 \times 10^{17}$ ion/cm² for $J = 2, 5, 8, 15,$ and 20 μ A/cm². The implantation was performed using an ILU-3 ion accelerator at room temperature of the bombarded substrate and for the normal incidence of the ion beam on the irradiated *c*-Si surface. For analyzing the Si sputtering with Ag⁺ ions and for determining effective sputtering ratio k for the implanted porous Ag : P*Si* layer, and interface (step) between the irradiated and unexposed sample regions was formed on the Si surface. For this purpose, ion implantation of *c*-Si was carried out through a copper–nickel mask (mesh with a size of 90 μ m and a period of 125 μ m), which was placed on the sample surface during irradiation. Experimental data on sputtering for each values of D and J were obtained from the measurements on five samples.

The morphology of the sample surface was investigated using a Merlin (Carl Zeiss) scanning electron microscope (SEM) with an In-Lens secondary-electron detector. For the same parameters of the electron microscope, but for the sample tilted relative to the probe beam direction through an angle of 70°, structural measurements were taken by the method of electron backscatter diffraction (EBSD) using a NordLys HKL detector (Oxford Instruments). The images of the transverse edge of the samples were recorded using a Hitachi SU 8230 SEM in the secondary electron detection regime. For this purpose, the sample was placed on the stage at an angle of 70° relative to the direction of the incident electron beam. Elemental analysis was performed on an X-Max energy-dispersion spectrometer (EDS) (Oxford Instruments) combined with the same microscope.

For observation of the detailed topology of the sample surface, we used a Dimension FastScan scanning probe microscope (SPM) (Bruker). Measurements were taken in the regime of quantitative nanomechanical mapping with probes having a rigidity of 0.4 N/m and a radius of curvature of about 5 nm. Optical images of implanted samples were also obtained using a Mikromed POLAR 1 optical microscope.

2. RESULTS AND DISCUSSION

As has been considered earlier in [19, 20], optical ellipsometry and EBSD data show that the surface Si layer formed by the implantation of Ag⁺ ions turns out to be amorphized completely even for a small dose $D \sim 1.3 \times 10^{14}$ ion/cm². By way of example, Fig. 1 shows the EBSD images for nonimplanted *c*-Si, as well as for that bombarded with $D \sim 1.3 \times 10^{14}$ ion/cm² and $J = 8$ μ A/cm². It can be seen from the figure that, in contrast to the initial sample, the EBSD of which is characterized by the pattern with the Kikuchi lines of the *c*-Si single crystal, the EBSD image for an Ag : Si sample exhibits only diffuse rings indicating the amorphization of the surface implanted layer. The emergence of the amorphous structure was also confirmed by the optical reflection spectra given in [21], where a decrease in the intensity at the peak of 268 nm down to 75% and complete disappearance of the band at 366 nm, which was initiated by the formation of the amorphous *a*-Si layer and the formation of the porous P*Si* surface during the implantation with $D = 1.5 \times 10^{17}$ ion/cm², were observed.

At the beginning of implantation, after breaking of the crystalline structure and amorphization of the implanted layer, the morphology of the bombarded Si surface leading to the formation of pores begins to change [15, 20]. As an example, Fig. 2 shows the SEM image of a transverse edge for an Ag : P*Si* sample formed at $D = 1.5 \times 10^{17}$ ion/cm² and $J = 8$ μ A/cm². The dark region in the lower half of the SEM image of the sample (see Fig. 2) corresponds to the end face part of the substrate of the initial *c*-Si sample. The upper part of the figure shows the surface at an angle. On this surface, open Si pores are observed. Large Ag nanoparticles (~40 nm) are distributed over the perimeter of the pore walls, while small nanoparticles (~7 nm) are distributed uniformly over the entire area of the sample.

As was mentioned in the Introduction, sputtering of the semiconductor surface was detected during the implantation of *c*-Si with Ag⁺ ions with a high value of $D = 1.5 \times 10^{17}$ ion/cm² [15, 16]. For determining the dependence of variation of thickness h of the sputtered layer on the ion bombardment duration (dose D), we performed a series of experiments with irradiation by Ag⁺ ions through a *c*-Si surface mask beginning with a small dose ($D = 1.5 \times 10^{15}$ ion/cm²).

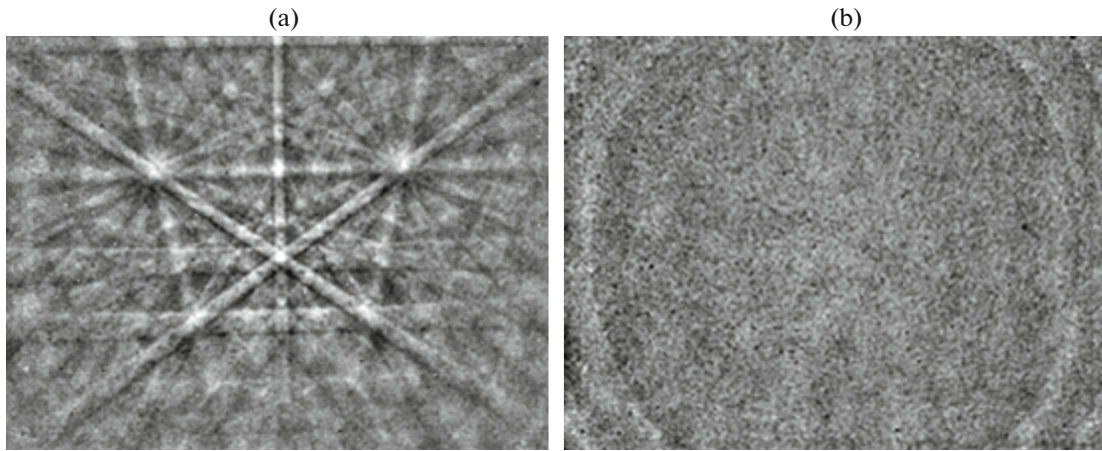


Fig. 1. RED patterns for (a) initial *c*-Si and (b) Si implanted with Ag^+ ions for $D = 1.3 \times 10^{14}$ ion/cm² and $J = 8 \mu\text{A}/\text{cm}^2$.

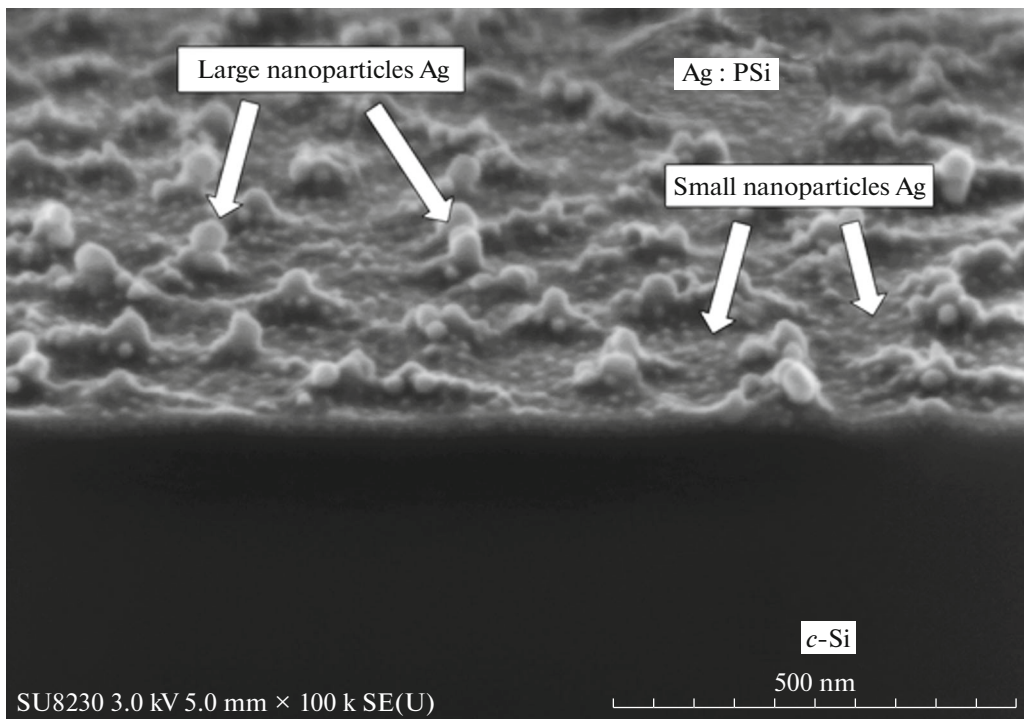


Fig. 2. SEM image of the transverse chip of Ag : P Si implanted with Ag^+ ions for $D = 1.5 \times 10^{17}$ ion/cm² and $J = 8 \mu\text{A}/\text{cm}^2$.

Figure 3a shows an example of the image obtained using an optical microscope for observing reflection from the Ag : P Si surface of the sample subjected to implantation with Ag^+ ion through a mask for the maximum used values of $D = 1.5 \times 10^{17}$ ion/cm² and $J = 8 \mu\text{A}/\text{cm}$. One can see a periodic structure with individual square meshes (light regions) on the sample surface, which has the same geometrical size as the applied mask (mesh; dark regions). The formation of the surface periodic structure as a result of implanta-

tion of *c*-Si with Ag^+ ions through the mask is also confirmed by the SEM image of the same sample (Fig. 3b).

We performed SPM measurements to observe a more detailed pattern at the boundary of the periodic structure formed by implantation on the sample surface and for obtaining numerical estimates of the formed profiles. The SPM images (Fig. 4) show a fragment of the periodic structure of the sample obtained for $D = 1.5 \times 10^{17}$ ion/cm² and $J = 8 \mu\text{A}/\text{cm}^2$. It can clearly be seen in the 3D SPM image (Fig. 4a) that the

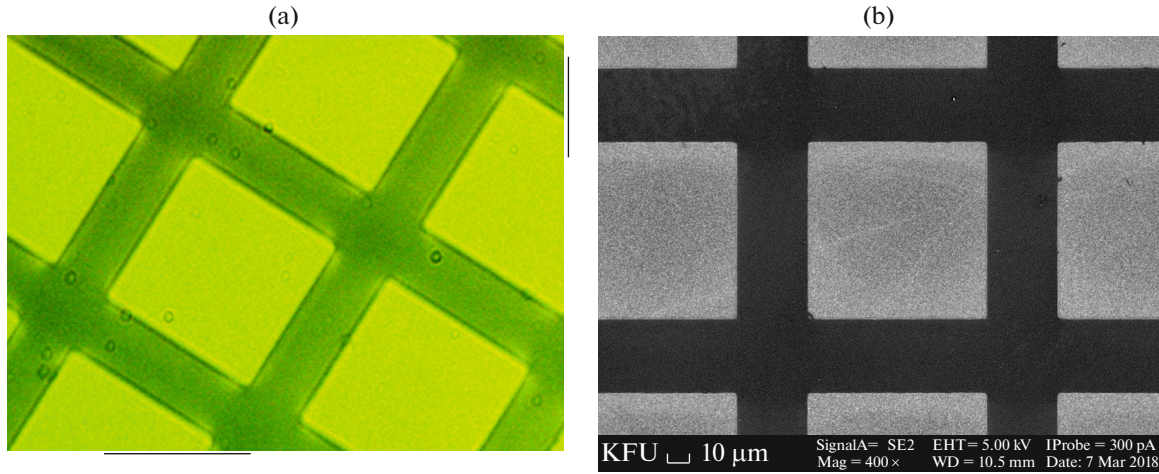


Fig. 3. (a) Optical microscope and (b) SEM images of the Si surface implanted through a mask with Ag^+ ions for $D = 1.5 \times 10^{17}$ ion/cm² and $J = 8 \mu\text{A}/\text{cm}^2$.

unimplanted *c*-Si surface in the form of the mesh wall (located under the mask during bombardment) rises above the ion-sputtered meshes. Judging from the colored scale shown on the right of the image of the region (see Fig. 4b), we can conclude that lighter regions correspond to the unimplanted (protected by the mask) sample region rising above the implanted square fragments of the sample (darker color hue). As noted above, a large-scale image makes it possible to perform quantitative measurements and to obtain estimates of dimensional parameters of formed meshes. By way of example, we have determined for the given sample the profile (Fig. 4c) measured across the mesh wall as shown by the line in Fig. 4b. It is found from this profile that $h = 60$ nm.

In experiments on ion implantation through a mask for different values of D and at constant $J = 8 \mu\text{A}/\text{cm}^2$, the formation of a step (sputtering) could be detected on SPM images with reasonable measurement error for the Ag : Si samples formed for $D \geq 2.5 \times 10^{16}$ ion/cm². Therefore, surface profiles were measured precisely for samples obtained in the interval of D values from 2.5×10^{16} to 1.5×10^{17} ion/cm², and the values of h were determined. Figure 5 shows the resultant $h(D)$ dependence for the Ag : Si surface implanted with the Ag^+ ions; it can be seen that the value of h increases monotonically and linearly with increasing D .

It follows from the above results that during the implantation of *c*-Si with Ag^+ ions, the sample surface is amorphized upon an increase in D (see Fig. 1) and becomes uneven and rough (see Fig. 2); it is also saturated with the Ag^+ ions that lead to the formation of Ag particles. Therefore, we cannot use sputtering ratio k for pure Si. However, the experimentally obtained values of h make it possible to determine effective sputtering ratio $k_{\text{eff}}(D)$ characterizing the Ag : Si samples

formed at various stages of ion implantation. It follows from the linear experimental profile shown in Fig. 5 that $k_{\text{eff}}(D)$ is constant. By definition, we have

$$k_{\text{eff}}(D) = \Delta n_{\text{Si}} / \Delta n_{\text{Ag}}, \quad (1)$$

where Δn_{Si} is the number of atoms knocked out from the bombarded material and Δn_{Ag} is the number of implanted Ag^+ ions participating in ion sputtering. For a specific D , we have

$$\Delta n_{\text{Si}} = \frac{\rho S \Delta h N_A}{M}, \quad (2)$$

where ρ is the Si density, S and Δh are the area and height of the implantation-sputtered layer, N_A is the Avogadro constant, and M is the molar mass of Si. Therefore, the estimated value is $k_{\text{eff}}(D) = 1.6$.

The measurements taken using such a technique for samples formed at constant $D = 1.5 \times 10^{17}$ ion/cm², but for different values of J , deserve special attention. Figure 6 shows experimental dependences $h(J)$ and $k_{\text{eff}}(J)$. Obviously, $k_{\text{eff}}(J)$ varies with J during the implantation of *c*-Si with Ag^+ ions.

According to the literature data [22], collision sputtering (also referred to as “physical” or “ion” sputtering), sputtering as a result of electronic processes (electron sputtering), and chemical sputtering are distinguished depending on the mechanism of occurrence of the process. In the case considered here, collisional sputtering during implantation is associated with a transfer of the kinetic energy from an accelerated ion (Ag^+) to atoms of the bombarded (Si) matrix; it dominates in the energy range of bombarding ions, in which elastic specific energy loss for impinging ions prevail (nuclear deceleration). As a result, some atoms acquire energy exceeding their binding energy with the surface and leave the target. During the implantation

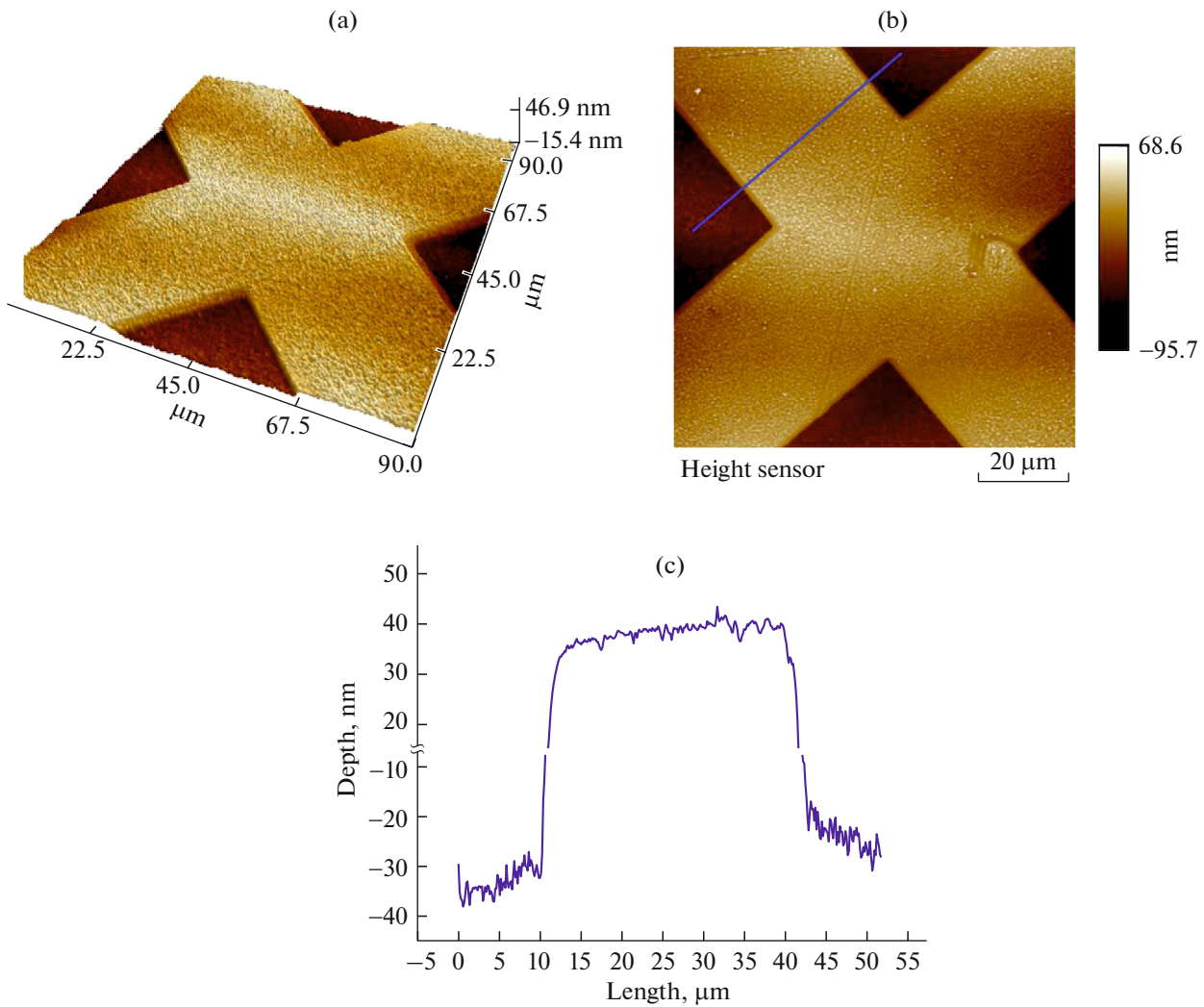


Fig. 4. (a) 3D and (b) 2D SPM images of the Si surface implanted through a mask with Ag^+ ions for $D = 1.5 \times 10^{17}$ ion/cm² and $J = 8 \mu\text{A}/\text{cm}^2$. The profile obtained by measuring across the cell wall (c), mesh wall as shown by the line in (b).

of Si with the Ag^+ ions with energy of 30 keV, this is the case when nuclear deceleration prevails; therefore, sputtering due to electronic processes caused by energy spent by electrons for excitation and ionization of Si atoms can be ignored. There is no need either to consider chemical sputtering associated with chemical reactions between bombarding Ag^+ ions and Si atoms (in view of their absence) with the formation of volatile compounds on the sample surface.

The theories of collisional sputtering are based on analysis of cascades of elastic collisions in irradiated matrices; in this case, three regimes are distinguished [22]. The first is the regime of direct knocking out of target atoms, which is realized during the implantation of targets with light ions. The lengths of cascades is small, and primarily knocked out atoms make a substantial contribution to sputtering. The second mechanism is called the “regime of linear cascades,” which

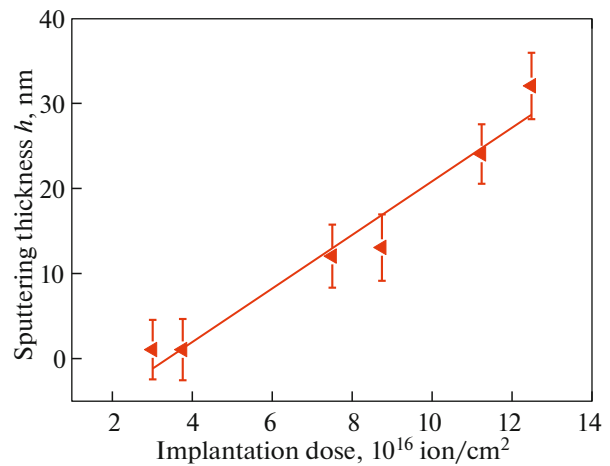


Fig. 5. Dependence of sputtering thickness h on implantation dose D for Ag : PSi samples formed at different values of D and fixed $J = 8 \mu\text{A}/\text{cm}^2$.

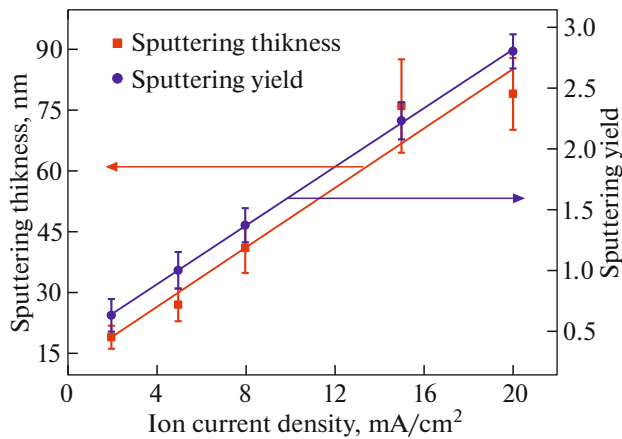


Fig. 6. Dependences of sputtering thickness h and sputtering yield on ion current density J for Ag : PSi samples formed at different values of J and fixed $D = 1.5 \times 10^{17}$ ion/cm².

is realized for most ions (except the heaviest ones) with energies from units to tens of kiloelectronvolts; this agrees with the energy of 30 keV used in our experiments. The density of distribution of target atoms knocked out from their equilibrium positions is low, so that collisions between moving atoms with stationary atoms of the irradiated matrix prevail, while collisions between moving atoms do not occur. The third mechanism is the regime of nonlinear cascades (thermal peaks, i.e., local heating of the bombarded material during energy transfer from an incident ion to target atoms). This is typical of ions with a large mass. The recoil atomic density distribution in the matrix is so high that most atoms within a certain (thermal peak) volume are in motion.

Obviously, for heavy Ag⁺ ions considered in this study, the first regime of sputtering is ruled out, and the observed processes must be characterized by cascade theories. It is difficult to give preference to linear or nonlinear regimes of cascades.

CONCLUSIONS

Thus, we have reported on the results of first experiments on sputtering of the implanted Si surface layer during its low-energy bombardment with Ag⁺ ions. For this purpose, we have worked out the precision technology of ion implantation through a mask and have developed a technique for quantitative SPM measurements and estimation of the resultant structures. It is found that with increasing ion dose D , the Si surface becomes amorphous and acquires a porous structure with silver nanoparticles formed in it. We have experimentally determined the $h(D)$ and $h(J)$ dependences. It has been shown that sputtering of implanted Si-based layer with an inhomogeneous

structure and chemical composition can be characterized by effective sputtering factor k_{eff} .

ACKNOWLEDGMENTS

Ion implantation was performed at the Kazan Zavoisky Physical Technical Institute, which is a separate structural branch of the Federal Research Center KazNTs of the Russian Academy of Sciences. Morphological analysis of test samples was carried out on the equipment of the Analytic Spectroscopy Interdisciplinary Center of the Kazan Federal University.

FUNDING

This study was supported by the Russian Science Foundation, project no. 17-12-01176.

CONFLICT OF INTEREST

The authors declare that they have no conflicts of interest.

REFERENCES

1. V. A. Milichko, A. S. Shalin, I. S. Mukhin, A. E. Kovrov, A. A. Krasilin, A. V. Vinogradov, P. A. Belov, and C. R. Simovski, *Phys.-Usp.* **59** (8), 727 (2016).
2. K. L. Chopra and S. R. Das, *Thin Film Solar Cells* (Springer, New York, 1983).
3. A. Polman, M. Knight, E. C. Garnett, B. Ehrler, and W. C. Sinke, *Science* **352**, add4424 (2016).
4. A. Polman, *Science* **322**, 868 (2008).
5. H. A. Atwater and A. Polman, *Nat. Mater.* **9**, 205 (2010).
6. U. Kreibig and M. Volmer, *Optical Properties of Metal Clusters* (Springer, Berlin, 1995).
7. A. L. Stepanov, *Ion Implantation Synthesis and Optics of Metal Nanoparticles* (Lambert Academic, Mauritius, 2018).
8. C. Rockstuhl, S. Fahr, and F. Lederer, *J. Appl. Phys.* **104**, 123102 (2008).
9. S. K. Sardana, V. S. N. Chava, and V. K. Komarala, *Appl. Surf. Sci.* **347**, 651 (2015).
10. K. V. Kozadaev, S. V. Leonchik, A. G. Novikov, O. V. Zinchuk, and L. V. Baran, *J. Appl. Spectrosc.* **83** (5), 776 (2016).
11. S. Chervinskii, A. Matikainen, A. Dergachev, A. Lipovskii, and S. Honkanen, *Nanoscale Res. Lett.* **9**, 398 (2014).
12. N. S. Yurova, N. E. Markina, M. V. Pozharov, A. M. Zakharevich, T. Yu. Rusanova, and A. V. Markin, *Colloids Surf., A*, No. 495, 169 (2016).
13. C. M. Lee, S.-P. Chang, S.-J. Chang, and C.-I. Wu, *Int. J. Electrochem. Sci.* **8**, 7634 (2013).
14. R. I. Batalov, V. I. Nuzhdin, V. F. Valeev, N. I. Nurgazov, A. A. Bukharaev, G. D. Ivlev, and A. L. Stepanov, *Opt. Spectrosc.* **126** (2), 144 (2019).

15. A. L. Stepanov, A. A. Trifonov, Y. N. Osin, V. F. Valeev, and V. I. Nuzhdin, *Optoelectron. Adv. Mater., Rapid Commun.* **7**, 692 (2013).
16. A. L. Stepanov, V. I. Nuzhdin, V. F. Valeev, V. V. Vorobev, A. M. Rogov, and Y. N. Osin, *Vacuum* **7**, 353 (2019).
17. M. Nastasi, J. W. Mayer, and J. K. Hirvonen, *Ion-Solid Interactions. Fundamentals and Applications* (Cambridge Univ. Press, Cambridge, 1996).
18. *Sputtering by Particle Bombardment*, Ed. by R. Behrisch (Springer, Berlin, 1981, 1983).
19. V. V. Bazarov, V. I. Nuzhdin, V. F. Valeev, V. V. Vorobev, Yu. N. Osin, and A. L. Stepanov, *J. Appl. Spectrosc.* **83** (1), 47 (2016).
20. V. V. Vorob'ev, A. M. Rogov, Yu. N. Osin, V. I. Nuzhdin, V. F. Valeev, K. B. Eidel'man, N. Yu. Tabachkova, M. A. Ermakov, and A. L. Stepanov, *Tech. Phys.* **64** (2), 195 (2019).
21. A. L. Stepanov, Y. N. Osin, V. V. Vorobev, V. F. Valeev, and V. I. Nuzhdin, *Optoelectron. Adv. Mater., Rapid Commun.* **11**, 685 (2017).
22. *Fundamental and Applied Aspects of Solid Material Sputtering*, Ed. by E. S. Mashkov (Mir, Moscow, 1989) [in Russian].

Translated by N. Wadhwa